

This paper has to be cited as: Díaz, E., Robles, P. & Tomás, R. 2018. Multitechnical approach for damage assessment and reinforcement of buildings located on subsiding areas: Study case of a 7-story RC building in Murcia (SE Spain). *Engineering Structures*, **173**, 744-757, doi: <https://doi.org/10.1016/j.engstruct.2018.07.031>

**MULTITECHNICAL APPROACH FOR DAMAGE ASSESSMENT AND  
REINFORCEMENT OF BUILDINGS LOCATED ON SUBSIDING AREAS: STUDY  
CASE OF A 7-STORY RC BUILDING IN MURCIA (SE SPAIN)**

E. Díaz<sup>1</sup>, P. Robles<sup>2</sup>, R. Tomás<sup>3</sup>

<sup>1</sup> Ph.D. Associate Professor, Departamento de Ingeniería Civil. Escuela Politécnica Superior, Universidad de Alicante, P.O. Box 99, E-03080 Alicante, Spain. [esteban.diaz@ua.es](mailto:esteban.diaz@ua.es)

<sup>2</sup> Ph.D. Associate Professor, Departamento de Ingeniería Civil. Escuela Politécnica Superior, Universidad de Alicante, P.O. Box 99, E-03080 Alicante, Spain. [pedro.robles@ua.es](mailto:pedro.robles@ua.es)

<sup>3</sup> Ph.D. Professor, Departamento de Ingeniería Civil. Escuela Politécnica Superior, Universidad de Alicante, P.O. Box 99, E-03080 Alicante, Spain. [roberto.tomas@ua.es](mailto:roberto.tomas@ua.es)

**Abstract**

The work presented herein proposes a multitechnical methodology for damage assessment and reinforcement of buildings located on areas affected by land subsidence induced by water withdrawal. The proposed methodology is illustrated by a comprehensive damage assessment and subsequent reinforcement of a 7-story reinforced concrete building located in the city of Murcia (SE Spain). Construction took place in the 1980's and the building was severely damaged by differential settlements caused by land subsidence throughout time. The building suffered an important tilting, presenting maximum settlement and tilt values of 260 and 177 mm, respectively, which considerably reduced its habitability and security conditions. Damage began to manifest in 1995, coinciding with an intense drought that affected the Murcia area between 1991 and 1995. Average piezometric level decreases of at least 8 m were verified, reaching 10 m in the nearby areas of the building. These piezometric level decreases caused important consolidation settlements that seriously damaged the structure of the building. The proposed multitechnical damage assessment methodology was used to characterize the causes of damage, design

This paper has to be cited as: Díaz, E., Robles, P. & Tomás, R. 2018. Multitechnical approach for damage assessment and reinforcement of buildings located on subsiding areas: Study case of a 7-story RC building in Murcia (SE Spain). *Engineering Structures*, **173**, 744-757, doi: <https://doi.org/10.1016/j.engstruct.2018.07.031>

reinforcement actions, and carry out subsequent monitoring to guarantee the structural stability of the building.

**Keywords:** Building damage; differential settlements; ground subsidence; building reinforcement; crack map; multitechnical approach.

## 1 **1. Introduction.**

2

3 Land subsidence caused by groundwater extraction is a human induced hazard that affects many  
4 cities and regions in the world (e.g. Hu et al. 2004; Phien-wej et al. 2006). Land subsidence can  
5 damage urban infrastructures, buildings and generally any structure in contact with the ground,  
6 due to its deformation. Damage is higher if ground deformation occurs differentially. Many cities  
7 around the world are located in subsiding areas, and therefore the buildings located within these  
8 areas are affected by ground movements that translate into loss of functionality, damage and in  
9 extreme cases, building failure (López Gayarre et al. 2010). Study and evaluation of such damage  
10 is especially relevant, with several published works regarding damage assessment schemes for  
11 buildings affected by subsidence (Cooper 2008; Del Soldato et al. 2017; Engineers 2000; Feng et  
12 al. 2008; Howard et al. 1993; Namazi and Mohamad 2013). These damage assessment schemes  
13 are based on are based on damage levels established by observation, and enable to define the  
14 degree of damage that a structure has suffered, according to a series of categories defined a priori.  
15 These categories relate the degree of damage with structural risk, without delving into more  
16 complex analyses on the techniques involving the study or mechanisms of damage.

17 Damage assessment schemes must be complemented by reinforcement or underpinning systems  
18 as well as concrete methodologies that collect data on the possible damage mechanisms,  
19 improving investigation and evaluation of such damage.

20 The overarching aim of this work is to propose a multitechnical approach for damage assessment  
21 and reinforcement of buildings located on subsiding areas. A study case is utilized to demonstrate  
22 the applicability of the method, consisting of a building with basement and 6 floors located in the  
23 urban area (Pintor Sobejano Street) of Murcia (SE Spain), affected by land subsidence. The  
24 building suffers severe problems due to differential settlements that endanger its habitability  
25 conditions.

26 The building is located on a subsiding area affected by groundwater withdrawal, known as the  
27 Vega of Murcia (Herrera et al. 2009; Jaramillo and Ballesteros 1997; Justo and Vázquez 2002;  
28 Rodríguez Ortiz and Mulas 2002; Tomás 2009; Tomás et al. 2005).

29 Subsidence involves the settlement of ground over a wide area, caused by natural or human-  
30 related factors (Corapcioglu 1984; Poland 1984). Subsidence can be classified according to the  
31 causing mechanisms (Scott 1978), being the subsidence caused by the extraction of fluids from  
32 the subsoil is one of the most important types of subsidence, and it affects important cities around  
33 the world (Galloway and Burbey 2011; Poland 1984). The extraction of water from an aquifer  
34 usually leads to a drop in the piezometric level, which can induce the consolidation of the affected  
35 layers, generating ground settlements. The case of Murcia was the first documented subsidence  
36 case in Spain related to a decrease in the piezometric level of the aquifer system called Vega  
37 Media and Baja del Segura. Land subsidence appeared during a prolonged drought period, which  
38 caused an overexploitation of the aquifer system.

39 Between 1975 and 1992, the piezometric level of this aquifer could be considered roughly  
40 constant (except for some variations under than 2-3 m). Between 1992 and 1995, a considerable  
41 decrease in the piezometric level was observed, with maximum values from 7.6 m to 10.8 m  
42 (Aragón et al. 2006). Data on subsidence settlements in Murcia during the piezometric crisis of  
43 the 1990s showed maximum values of up to 30 cm (Jaramillo and Ballesteros 1997). These  
44 settlements occurred mainly between 1992 and 1995, in the city of Murcia, and affected more  
45 than 150 buildings and other structures, entailing costs over 50 million Euros (Mulas et al. 2003;  
46 Rodríguez Ortiz and Mulas 2002).

47

## 48 **2. Common damage in buildings located on subsiding areas due to groundwater withdrawal.**

49

50 The damage suffered by buildings located on subsiding areas varies according to different factors  
51 related to the building itself and to the subsoil, such as load asymmetry, coexistence of different  
52 types of foundations, variation of the thickness of soft soil layers, to name a few.

53 The relative stiffness of concurrent elements (soil, foundation and superstructure) can also  
54 influence subsidence. Subsidence causes damage to buildings by the following mechanisms:

- 55 • Absolute settlements, which are always present and are precursors of damage  
56 (although this can be negligible);

- 57           •       Differential settlements, which generate significant damage in the case of isolated  
58           and poorly rigid foundations and / or significant heterogeneities in the ground or the loads.
- 59           •       Tilts, in relatively rigid foundations with also rigid structures. Tilts can be quite  
60           spectacular without affecting excessively the mechanics of the structure (but functionality  
61           is seriously affected).
- 62           •       Structural failure of the foundation, in very specific cases only, such as end-  
63           bearing piles with a low failure safety factor, when a great negative skin friction is  
64           generated, or in foundations with non-isolated but relatively flexible, when deformations  
65           are significant.

66 Table 1 shows the types of foundations usually utilized, in decreasing order of damage  
67 probability.

68

Type of foundation	Relative damage			
	Absolute settlements	Differential settlements	Tilts	Structural failure of the foundation
Isolated footings	xxxxx	xxxxx	xx	x
Friction piles	xxxxx	xxxxx	xx	x
Stripped footings	xxx	xxx	xxx	xxx
Flexible slabs	xxx	xxx	xxxx	xxx
Rigid slabs	xxx	x	xxxxx	xx
End bearing piles	x	x	x	xxx



69 *Table 1. Vulnerability to subsidence, for the most common types of foundations. Magnitude of damage: xxxxx very*  
70 *important, xxxxx important, xxx intermediate, xx reduced, x negligible.*

71

72

73 **3. Description of the building.**

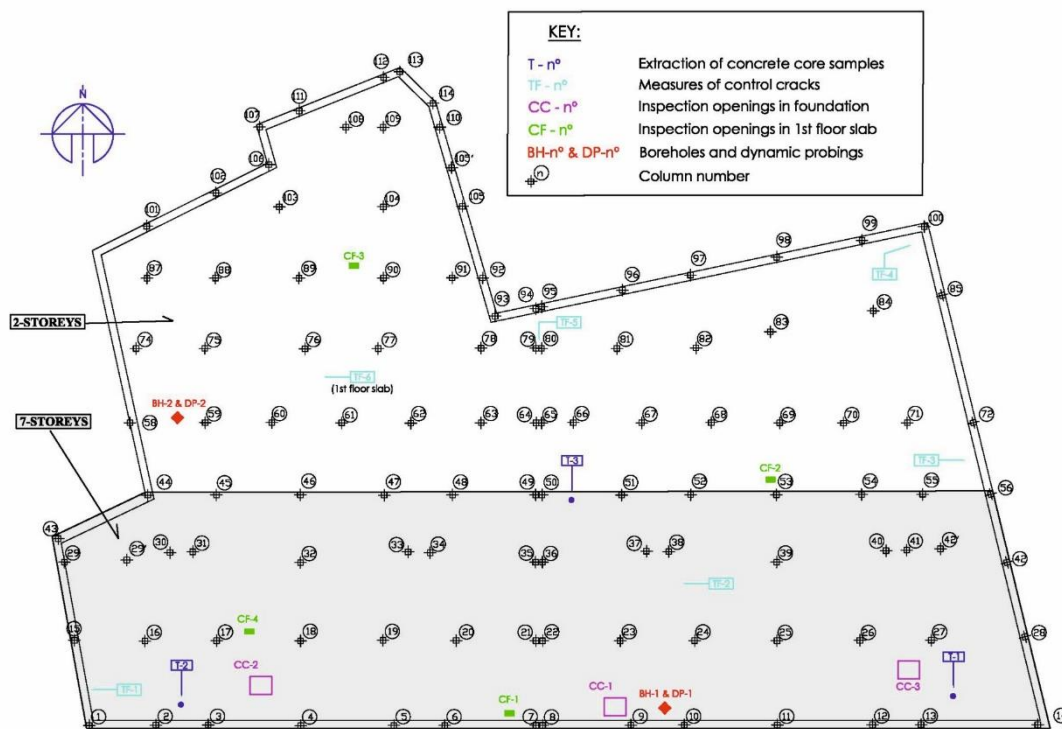
74

75 The gross floor area of the building is 1861 m<sup>2</sup> (Figure 1). This area is fully occupied by parking  
76 in the basement, and is divided into two different zones, starting from the ground floor: a) the first  
77 zone is founded on isolated footings and has not been strongly affected, and b) the second zone

78 presents six stories and is founded on reinforced concrete ribbed raft foundation, 30 cm height  
 79 with 0.50 x 0.80 m (width x height) beam stiffeners, aligned with the porticoes parallel to the  
 80 main façade.

81 Regarding the structural disposition, the two areas are divided by a transverse expansion joint that  
 82 separates the building into two independent structures. The structure presents one-way spanning  
 83 slabs of prestressed semi resistant joists and precast concrete hollow flooring bricks, supported  
 84 by 30 cm height reinforced concrete beams, parallel to the main façade and over columns of the  
 85 same material. The asymmetric shape of the building results in that the clear span between  
 86 columns can present heterogeneous values, ranging from 4 m to almost 7 m in the third portico.

87 This fact, together with the difference in height between the two areas of the aforementioned  
 88 building, causes asymmetry in the distribution of loads, where the most heavily-loaded columns  
 89 are those surrounding the South façade.



90  
 91 *Figure 1. Basement plan of the building with the location of the tests developed. The shadowed area corresponds to*  
 92 *the 7-storey zone of the building.*

93  
 94

#### 95 **4. Forensic investigation.**

96

97 Forensic investigation started in June 2008 and concluded in March 2013, when structure  
98 monitoring was carried out, comprising four groups of actions:

99

100 • Those related to the verification, inventory and classification of the damage  
101 observed during visits to the building.

102 • Works carried out to determine the geotechnical characteristics of the foundation  
103 ground of the building.

104 • Those related to structure, consisting of the measurement of deformations,  
105 installation of crack monitors, extraction and testing of concrete test specimens and the  
106 execution of openings in foundation and floor slabs.

107 • Those related to structure monitoring after underpinning, which will be discussed  
108 in detail in section 7.

109

110 Each action carried out is described next.

111

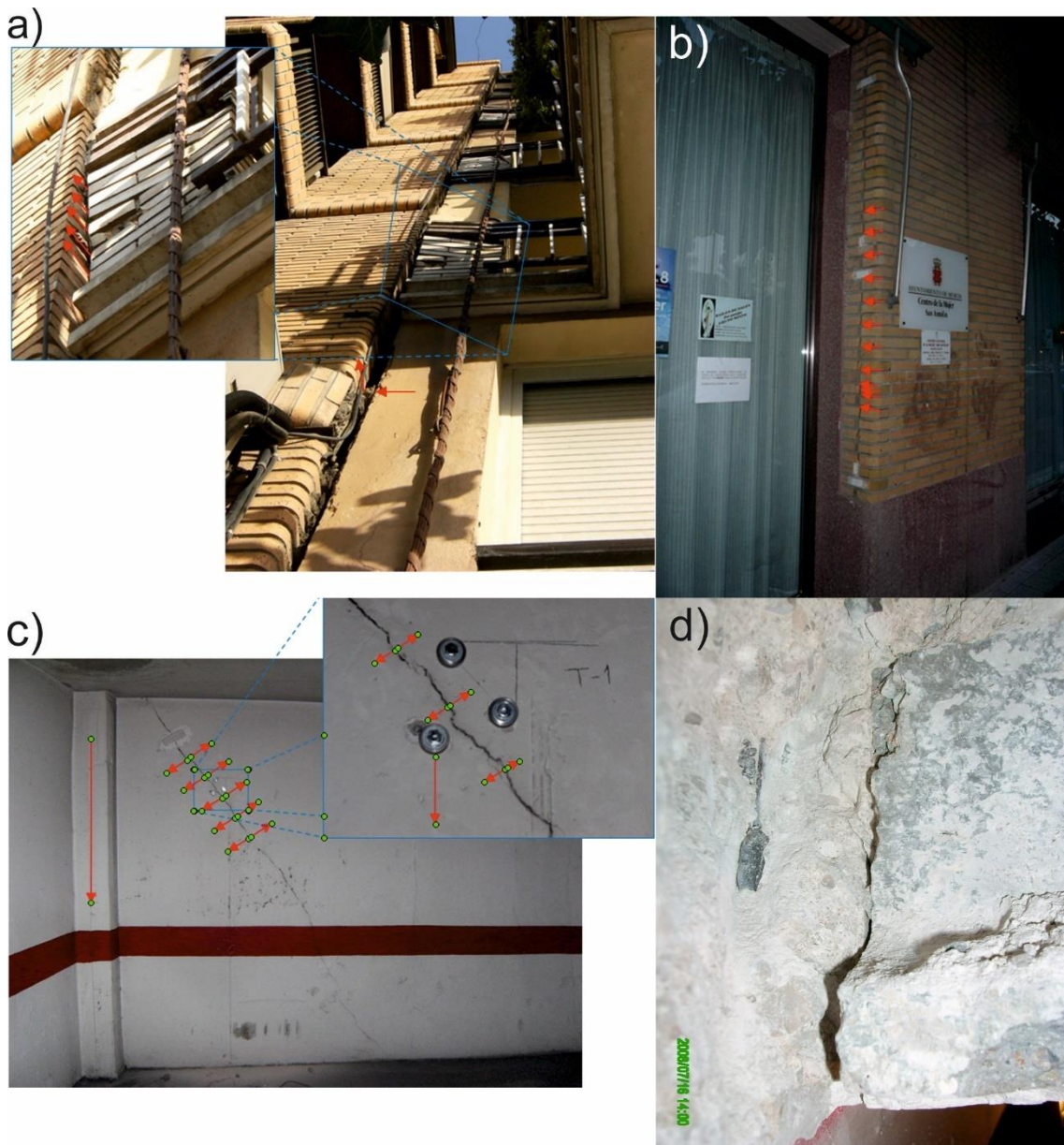
#### 112 **4.1. Building inspections. Observed damage.**

113

114 The inspections revealed damage due to an important tilt of the building towards its main façade  
115 (South) simultaneously to the existence of various crack patterns of different elements (e.g.,  
116 widespread cracking of the concrete slab and walls of the basement, isolated cracking of some  
117 vertical and horizontal elements, etc.).

118 The tilt of the main façade is noticeable to the naked eye because, at the height of the rooftop  
119 floor, 115 and 177 mm displacements have been registered in the SW and SE directions  
120 respectively, with respect to the base. These displacements are also evident when comparing the  
121 adjacent façades vertically (Figure 2a).

122



123

124 *Figure 2. a) Details of the collapse of the study case building and of the mismatch with the adjacent building due to*  
 125 *interaction between buildings. b) Vertical cracking of façade bricks due to excessive compression stress. c) View of*  
 126 *the crack on the South end of the West wall and detail of the pins installed for crack control. d) Inspection opening on*  
 127 *the first-floor slab (code R-2), where it was verified that the semi resistant joist is suspended and therefore does not*  
 128 *fulfil its objective.*

129

130 Vertical cracks were verified in the façade bricks of some walls, which started at street level until  
 131 reaching the second-floor slab (Figure 2b).

132

133

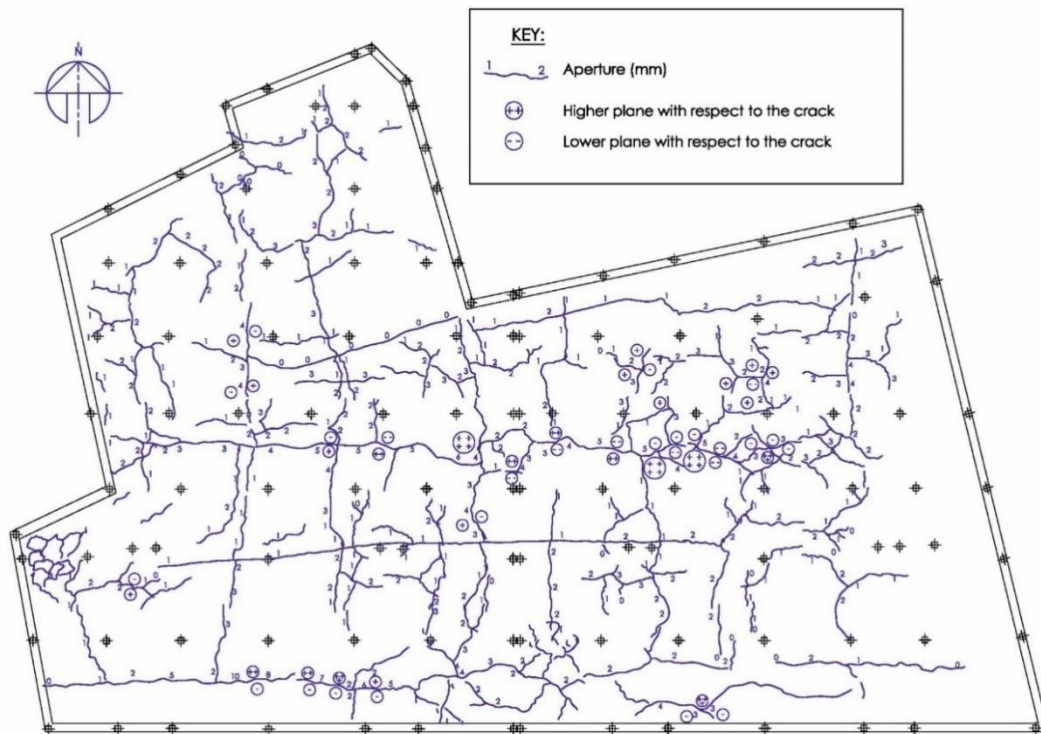


134 In the basement, the walls perpendicular to the façades present 45° sloping cracks increasing in  
135 height and opening towards the main façade (Figure 2c). Still in the basement, large sections  
136 presented zigzagging cracks at the base of the first-floor slab, in the joist-beam embedment area  
137 (Figure 2d), as well as some fine rectilinear fissures (transverse lines) between the porticoes. The  
138 slab of the basement (parking) also presented generalized cracking, where longitudinal cracks can  
139 be highlighted, practically parallel to the main façade, running from one wall to the opposite,  
140 coinciding with the equidistant space between the different porticoes. Figure 3 shows a detailed  
141 map of the cracks observed in the basement. There are other less important cracks for which  
142 description is omitted due to the negligible contribution herein.

143

144 Construction of the building began in September, 1983 and lasted until April, 1986. The first  
145 visible damage appeared in 1995, coinciding with the drought that occurred in the Vega of Murcia  
146 between 1991 and 1995 .

147



148

149

Figure 3. Map of the cracks detected on the basement floor.

150

151 **4.2. Geotechnical conditions.**

152

153 Two boreholes were made by a rotating drill system, with continuous core extraction (location  
 154 shown in Figure 1) to determine the geotechnical conditions of the site. Investigation continued  
 155 with two dynamic super heavy probes (DPSH). The most relevant properties of each geotechnical  
 156 unit are shown in Table 2.

157

158 During the execution of boreholes (July 3, 2008), the water table was located at 10.5 m below the  
 159 street level. Nearby municipal wells provided information on the recent variations of the  
 160 piezometric level of the zone: on average, that the position of the water table in 1983 was  
 161 approximately 3 m below the street level, and in 1995, was 13 m below the street level.

162

163 Figure 4 shows the geotechnical profile of the subsoil.

164

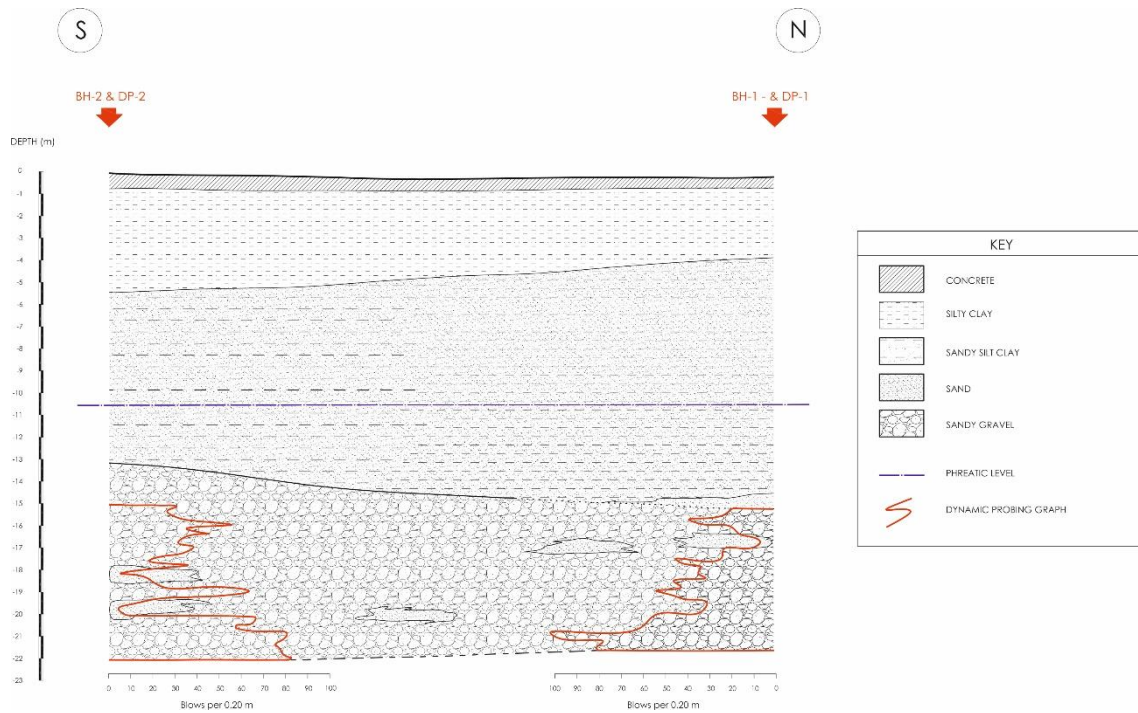
Unit	Depth (m)	USCS	Pass 0.08 mm (%)	N <sub>30</sub>	q <sub>u</sub> (kPa)	LL / PI	γ <sub>d</sub> (kN/m <sup>3</sup> )	w (%)	c' (KPa)	φ' (°)	e <sub>0</sub>	c <sub>c</sub>
I. Silty clay	0.0 - 3.65/5.40	CL or ML	79-90	5-16	--	39.4/18.4	--	21.7	--	--	0.80	0.24
II. Sandysilt clay	3.65/5.40 - 15.00/13.10	CL or ML or SM	85-98	0-5	38-140	37.6/19.2	16.5	28.1	15	25	0.73	0.18
III. Sandy gravel	15.00/13.10 - End	GW	2.3	35-R*	--	--	--	--	0	41	--	--

165 *Table 2. Geotechnical properties of the subsoil. With, USCS: Soil classification according to USCS. Pass 0.08 mm: pass through*  
 166 *0.08 mm sieve. N<sub>30</sub>: Result of Standard Penetration Test. q<sub>u</sub>: uniaxial compressive strength. LL: Liquid limit. PI: Plasticity Index. γ<sub>d</sub>:*  
 167 *dry density. w = water content. c': effective cohesion. φ': effective internal angle of friction. e<sub>0</sub>: initial void ratio. c<sub>c</sub>: compression*  
 168 *index. \*N<sub>20</sub>: Result of Dynamic Probing Super Heavy.*

169

170

171



172

173 *Figure 4. Geotechnical profile of the subsoil under the study case building. The silty clay level presents a slight southward dip. The*  
 174 *location of boreholes is shown in Figure 1.*

175

176 **4.3. Works in the structure.**

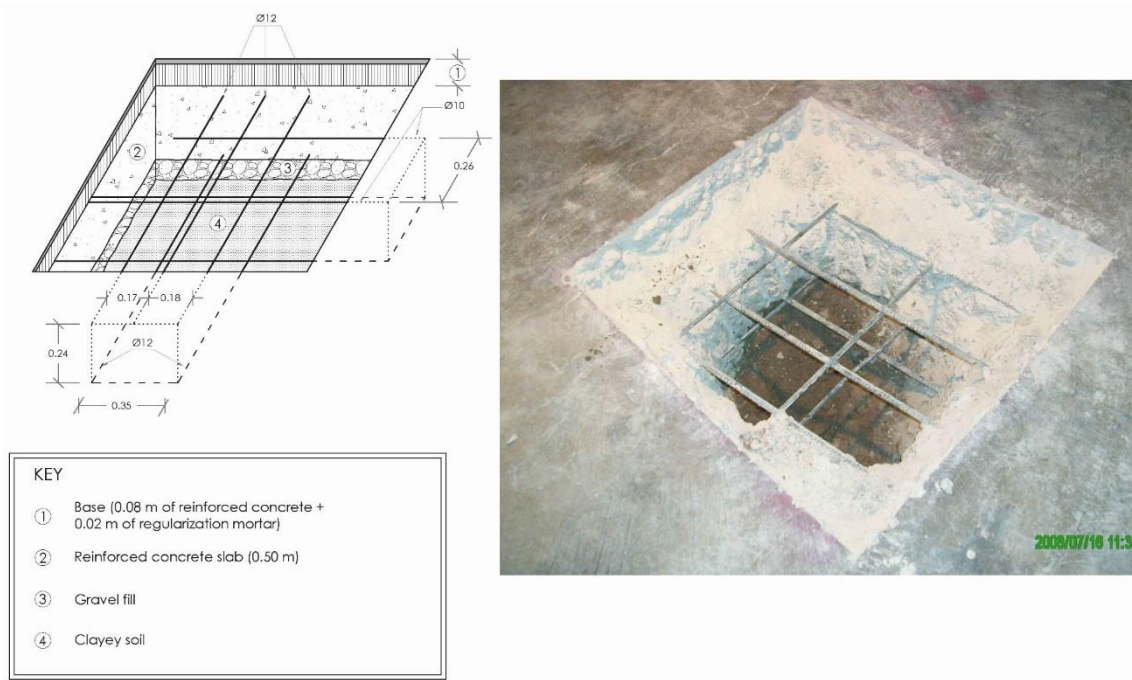
177

178 **4.3.1. Inspection openings.**

179

180 For an adequate evaluation of the dimensions, constructive procedures, damages and / or  
 181 deficiencies of a selection of hidden elements of the structure, a series of inspection openings  
 182 were made for the establishment of real dimensions and reinforcements. These data were then  
 183 compared with those indicated in the original drawings and subsequently utilized in the  
 184 calculation of the proposed reinforcement solution. In total, three inspection openings were made  
 185 in the foundation, with locations shown in Figure 1, demonstrating that the dimensions and  
 186 reinforcements of the project were fulfilled. An example of the procedure carried out is shown in  
 187 Figure 5.

188



189

190 *Figure 5. Inspection opening performed in the slab foundation (code CC-3). See location of inspection openings in Figure 1.*

191

192 On the other hand, the cracks observed in the links of the joist of the first-floor slab with their  
 193 respective main beams (Figure 2d) as well as some open cracks between the floor tiles (near and  
 194 parallel to the main façade) indicate the existence of tension stresses as origin of its displacement.  
 195 Four inspection openings were made in the first-floor slab (see location in Figure 1) and it was  
 196 confirmed that the first-floor slab was built with prestressed joist. Regarding the joist-beam  
 197 embedment in the points investigated, unequal embedment measurements were obtained (shown  
 198 in Table 3). A detail of the inspection opening between pillars 89 and 90 is depicted in Figure 6.

199

<b>Support of the precast semi resistant joist of the 1st floor slab</b>				
Inspection opening	CF-1	CF-2	CF-3	CF-4
Embedment length (cm)	5.8	-0.3	-1.3	2.5

200

201 *Table 3. Embedment length of the precast semi resistant joist and respective main beams, in the 1st floor slab. Positive values*  
 202 *indicate embedment or contact with support on the main beam, while negative values indicate the minimum separation between the*  
 203 *ends of the joist and its support on the beam.*

204



205

206

207

208

*Figure 6. Inspection opening on the first-floor concrete slab (code CF-3 in Figure 1). A detachment of 1.3 cm between the semi resistant joist and the main beam was registered.*

#### 209 **4.3.2. Determination of displacements.**

210

211 Displacements were measured to determine the magnitude of the movements experienced by the  
212 building. These data will be utilized to determine the type of movement (tilt and settlement,  
213 differential or in block) that the structure has experienced. To this end, the actions described next  
214 were carried out.

215

##### 216 *4.3.2.1. Topographic levelling of the basement floor.*

217 Precision levelling of the column bases and perimeter walls was carried out to establish the  
218 topography of the upper side of the foundation slab. These data were compared with planimetric  
219 data provided by the drawings of the project, enabling determination of the topography of the  
220 basement floor and deduction of the local descents of the analysed points. A representation of the  
221 analysis is shown in Figure 7a.

222

223

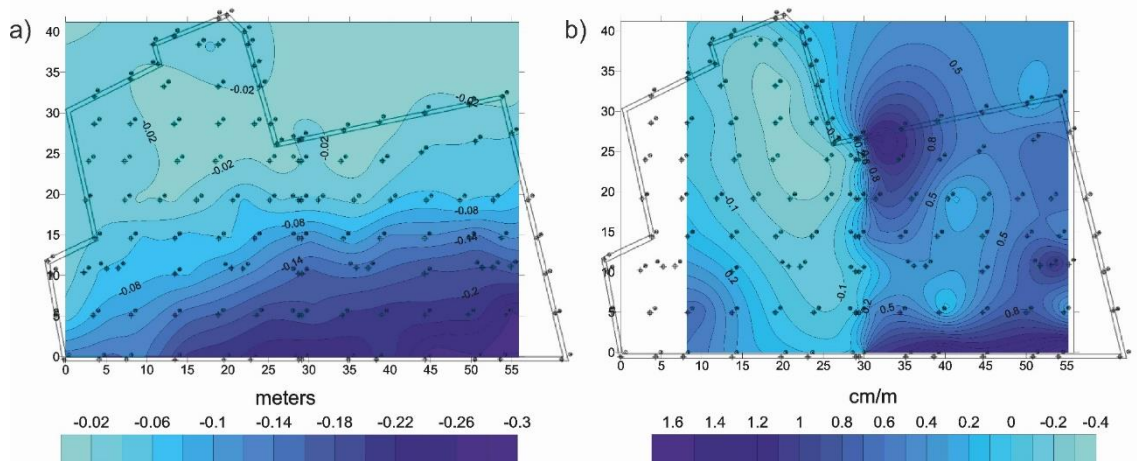


224 4.3.2.2. Calculation of tilts.

225

226 Tilt measurements were analysed in various elements of the structure to determine the type of  
227 turning movement and possible structural repercussions. The overall tilt of the columns in the  
228 basement floor was checked, and the results are represented in Figure 7b.

229



230

231

Figure 7. a) Topography of the upper side of the foundation slab. b) Tilt of columns in the basement floor.

232

233 Figures 7a and 7b show that significant deformations are concentrated on the South end of the  
234 building, with settlement values slightly above 260 mm.

235

236 4.3.2.2. Angular distortions.

237

238 The structural system of the building presents porticoes parallel to the main façade (even the  
239 foundation slab is ribbed in that direction with greater height). Angular distortions were  
240 determined as the difference between the vertical displacements corresponding to contiguous  
241 columns in the direction of the frame and the separating distance. Seventy-one columns  
242 (considered as simple porticoes) were evaluated and grouped into four categories (shown in Table  
243 4). Figure 8 depicts the plant representation of the obtained values.

244

245

Group	Angular distortion	N° of columns/ % of total	Risk of cracking partitions	Risk of structural damage
1	<1/500	32 / 45%	Low	Negligible
2	1/500-1/300	11 / 16%	Moderate	Low
3	1/300-1/150	18 / 25%	High	Moderate
4	>1/150	10 / 14%	Very high	High

246

*Table 4. Results of the angular distortion study and classification according to the Burland et al. (1977) criterion.*

247

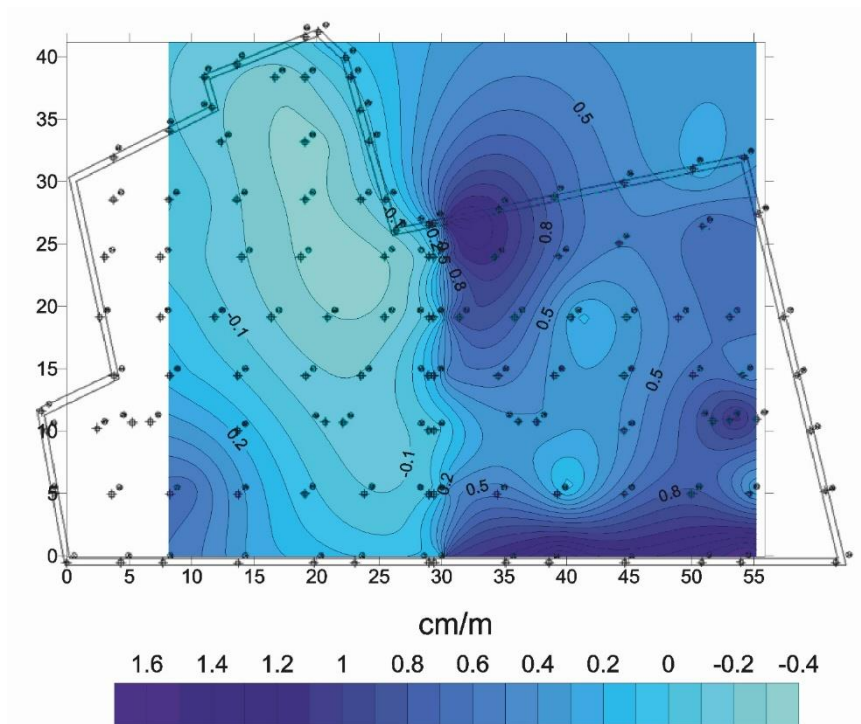
248 The results presented in Table 4 are congruent with the crack map of the building and it is

249 noteworthy to mention that areas with high absolute deformation (right lower quadrant of Figure

250 7a) present zones with small angular distortions, indicating that the turning movement of the

251 building has been, mostly, as a rigid solid.

252



253

254

*Figure 8. Angular distortions of the basement floor columns.*

255

#### 256 4.4. Cracks control

257

258 Six pins were placed at selected representative cracks to analyse their movement; pins were

259 attached to each side of the crack and arranged in a triangular configuration. Tracking of the

260 distance between points with known relative coordinates enables the determination of magnitude,

261 direction, sense and temporal variation of movements. Figure 2c shows a detail of the type of

262 control utilized. In addition, the specific locations of the crack control systems are shown in Figure  
 263 1. Table 5 presents control data prior to underpinning.

264

Reading date	X Axis														
	Displacement (0.1mm)					Velocity (0.1mm/day)					Acceleration (0.1 mm/day <sup>2</sup> )				
	T-1	T-2	T-3	T-4	T-5	T-1	T-2	T-3	T-4	T-5	T-1	T-2	T-3	T-4	T-5
7-aug-08	---	---	---	---	0.00	---	---	---	---	0.000	---	---	---	---	0.000
25-aug-08	---	---	---	---	0.10	---	---	---	---	0.006	---	---	---	---	0.003
18-sep-08	---	---	---	---	1.10	---	---	---	---	0.042	---	---	---	---	0.015
2-oct-08	---	---	---	---	3.40	---	---	---	---	0.160	---	---	---	---	0.084
16-oct-08	---	---	---	---	2.40	---	---	---	---	-0.070	---	---	---	---	-0.164
28-oct-08	---	---	---	---	2.30	---	---	---	---	-0.009	---	---	---	---	0.050
10-nov-08	---	---	---	---	7.90	---	---	---	---	0.432	---	---	---	---	0.339
21-nov-08	---	---	---	---	9.00	---	---	---	---	0.103	---	---	---	---	-0.299

265

Reading date	Y Axis														
	Displacement (0.1mm)					Velocity (0.1mm/day)					Acceleration (0.1 mm/day <sup>2</sup> )				
	T-1	T-2	T-3	T-4	T-5	T-1	T-2	T-3	T-4	T-5	T-1	T-2	T-3	T-4	T-5
7-aug-08	0.00	0.00	0.00	0.00	0.00	0.000	0.000	0.000	0.000	0.000	0.000	0.000	0.000	0.000	0.000
25-aug-08	-0.40	-0.40	-0.30	0.30	-1.00	-0.023	-0.020	-0.016	0.014	-0.053	-0.013	-0.011	-0.009	0.008	-0.030
18-sep-08	-0.80	-0.90	-0.70	0.70	-2.20	-0.014	-0.022	-0.016	0.017	-0.050	0.004	-0.001	0.000	0.001	0.001
2-oct-08	-0.80	-0.80	-0.90	1.10	-1.60	-0.005	0.008	-0.013	0.029	0.039	0.006	0.022	0.003	0.009	0.064
16-oct-08	-1.00	-0.50	-1.00	1.00	-0.90	-0.015	0.018	-0.009	-0.005	0.050	-0.007	0.007	0.003	-0.024	0.008
28-oct-08	-0.80	0.00	-0.90	1.30	0.00	0.019	0.046	0.006	0.029	0.079	0.029	0.023	0.013	0.029	0.024
10-nov-08	-1.10	-0.30	-1.10	2.40	-1.00	-0.020	-0.027	-0.018	0.079	-0.079	-0.030	-0.056	-0.018	0.039	-0.122
21-nov-08	-1.40	0.10	-1.60	2.80	-2.20	-0.028	0.036	-0.039	0.036	-0.109	-0.007	0.057	-0.020	-0.039	-0.028

266

Reading date	Z Axis														
	Displacement (0.1mm)					Velocity (0.1mm/day)					Acceleration (0.1 mm/day <sup>2</sup> )				
	T-1	T-2	T-3	T-4	T-5	T-1	T-2	T-3	T-4	T-5	T-1	T-2	T-3	T-4	T-5
7-aug-08	0.00	0.00	0.00	0.00	---	0.000	0.000	0.000	0.000	---	0.000	0.000	0.000	0.000	---
25-aug-08	0.00	0.20	0.10	-0.50	---	-0.002	0.013	0.007	-0.025	---	-0.001	0.007	0.004	-0.014	---
18-sep-08	0.20	-0.10	0.20	-0.80	---	0.011	-0.014	0.005	-0.013	---	0.005	-0.011	-0.001	0.005	---
2-oct-08	0.10	-0.10	0.20	-1.10	---	-0.006	-0.003	-0.007	-0.022	---	-0.012	0.008	-0.008	-0.007	---
16-oct-08	-0.10	0.10	0.00	-1.10	---	-0.019	0.015	-0.014	-0.005	---	-0.009	0.013	-0.005	0.012	---
28-oct-08	-0.20	-0.40	0.30	-0.90	---	-0.003	-0.040	0.025	0.017	---	0.014	-0.046	0.033	0.018	---
10-nov-08	-0.30	0.10	0.30	-1.80	---	-0.012	0.038	0.001	-0.063	---	-0.007	0.059	-0.019	-0.061	---
21-nov-08	-0.40	-0.20	-0.20	-2.10	---	-0.005	-0.027	-0.045	-0.028	---	0.007	-0.058	-0.041	0.031	---

267 *Table 5. Results of cracks control. Vertical Z axis corresponds to upward positive direction. Only readings from controls 1*  
 268 *to 5 are shown, as control 6 was utilized exclusively in the monitoring phase.*

269

270 Comparison of obtained data enabled determination of the correlation across the different quantified  
 271 movements. Pearson's correlation coefficient is a statistical parameter that analyses two vectors and  
 272 expresses their relationship by assigning a value between 1 and -1 (1 = direct relationship, 0 =



273 unrelated, -1 = inverse relationship). Herein all correlation coefficients were found between 0.91 and  
274 0.99, which indicates a high degree of correlation between the movements of all cracks, suggesting  
275 that the cause was the same.

276

#### 277 **4.5. Concrete sampling**

278

279 The extraction points for concrete sampling were selected considering statistical and  
280 representativeness criteria. At each selected location of the foundation slab, three cylindrical concrete  
281 core samples were extracted (Figure 1) for subsequent uniaxial compressive strength tests. These  
282 tests are necessary for the design and calculation of the proposed reinforcement, providing  
283 information about the quality and state of the existing concrete. All obtained results were higher than  
284 25 MPa (minimum uniaxial compressive strength required in the original project).

285

#### 286 **5. Finite Element Method analysis.**

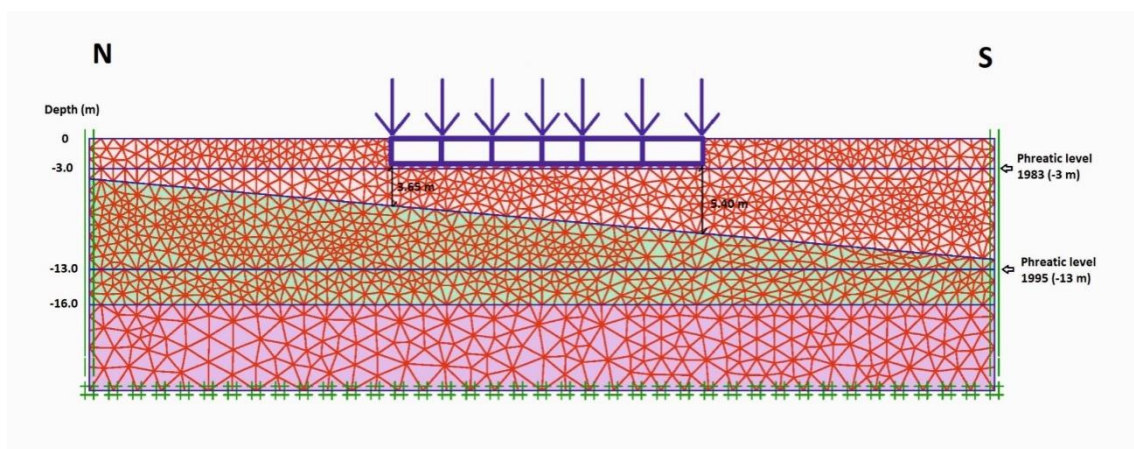
287

288 A comprehensive structural and geotechnical analysis was developed, using the Finite Element  
289 Method (FEM), to determine the causes of the observed damage. Analysis considered the actual  
290 loads of the building and the previously described load asymmetry. A transversal section of the  
291 structure was modelled, perpendicular to the main façade, considering two different computation  
292 phases: a) an initial phase with the phreatic level located at -3 m below ground surface (ground  
293 water level when construction of the building was finished); and b) a final phase with the phreatic  
294 level located at -13 m below ground surface (maximum registered depth). Finally, the settlements  
295 associated with the consolidation process caused by water level decrease between both phases  
296 was calculated. Figure 9 shows the model adopted for the calculation of settlements.

297

298 The obtained results provided a maximum settlement of 230.6 mm, located at the South zone of  
299 the building. This value is similar to those obtained via levelling at the upper side of the foundation  
300 slab of the building (Figure 7a), confirming the relative rotation of the building on the same

301 direction and magnitude as observed in situ. It can be concluded that the decrease of groundwater  
302 level registered across the valley was the main cause of the observed damage. Modelling of the  
303 first phase (i.e., 1983 groundwater level) did not explain the magnitude of the observed damage,  
304 although it revealed the beginning of the rotation of the building. Rotation was probably due to  
305 the concentration of stress on the area under the façade of the building, which increased the  
306 settlement of the area as the groundwater table decreased to its minimum value registered in 1995  
307 (modelled in the second phase).  
308



309  
310 *Figure 9. Finite Element Model of the studied building. The geotechnical properties of the different layers are described in detail in*  
311 *section 4.2.*

312  
313 The asymmetry of the loads on the slab foundation and the different thickness of the compressible  
314 soil layer (i.e., silty clays), combined with groundwater level decrease, have caused the building  
315 to rotate in the direction of the main façade (South) with similar tilts in the N and S façades  
316 (approximately 1.0%) and with horizontality losses on the building floors. As the structure is  
317 founded by a reinforce concrete slab, the effect of differential settlements on the structure has  
318 been considerably limited. The rotation axis of the building is almost parallel to the façades, being  
319 slightly rotated in the left-hand direction. This has caused the building to lean against the East  
320 neighbour building. Consequently, horizontal stress has been transmitted to the neighbour  
321 building, causing breakage of panels and tiles due to the induced compression. Damage has

322 progressed due to the insufficient rigidity of the foundation against a rotation process of this  
323 magnitude.

324

325 **6. Description of the reinforcement solution adopted.**

326

327 The reinforcement system encompassed actions on the structure, with steel angle (“L” laminated  
328 profiles) reinforcements installed between the main beams and the semi resistant joists. Actions  
329 on the foundation were also carried out, underpinning the foundation with micropiles to end its  
330 movements. Before underpinning the foundation, steel angles were placed in the porticoes of the  
331 building (Figure 10) to reinforce the connections between the main beams and the semi resistant  
332 joists.

333



334

335

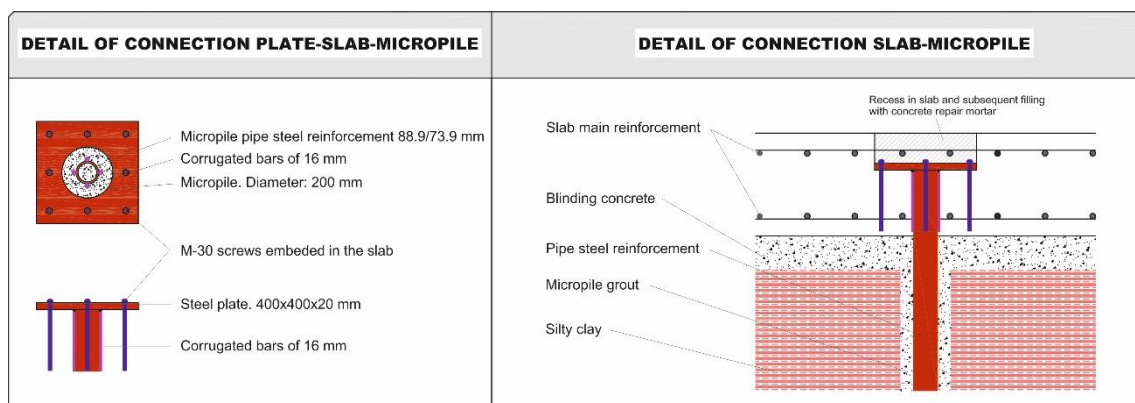
*Figure 10. Detail of the steel angle reinforcements between the semi resistant joists and main beams.*

336

337 Due to the characteristics of the ground within its first meters and the existing foundation, any  
338 type of superficial underpinning of the foundation was discarded. Deep underpinning with  
339 micropiles was executed, which transmitted the loads of the existing shallow foundation to the  
340 deeper gravel level (Level III).

341 The underpinning works finished in June, 2010. The micropiles were connected to the existing  
342 foundation by anchor plates. The adopted solution consisted of two to five micropiles per column,  
343 depending of the load. The micropiles had a drill diameter of 200 mm and were reinforced by a  
344 88.9/73.9 mm steel pipe (outer/inner diameter). In the upper sections of the steel pipe, four  
345 corrugated steel bars (16 mm diameter) were welded to improve adhesion between the micropiles  
346 and the existing foundation (Figure 11). Finally, the embedded micropiles and the slab recess  
347 were completely filled with concrete repair mortar.

348



349

350 *Figure 11. Detail of the connection between the existing foundation and the embedded micropiles.*

351

352 One hundred and fifty-five micropiles were drilled, with variable lengths (16.5 or 21.0 m),  
353 according to the supported load.

354

## 355 **7. Validation of the reinforcement solution through settlement monitoring.**

356

- 357 • Once the underpinning of the building was finished, a structural monitoring plan was  
358 formulated to verify the suitability of the adopted remedial measures. The plan  
359 contemplated three measures:

- 360 • Monitoring of the relative settlement between the columns located within and outside the
- 361 reinforced area.
- 362 • Monitoring of the crack control pins at different sectors of the building, to characterize
- 363 the movements using a calliper (Figure 2c).
- 364 • Monitoring of the groundwater level under the building.

365

366 The levelling carried out between 2008 and 2013 indicated that the elevation increments of the

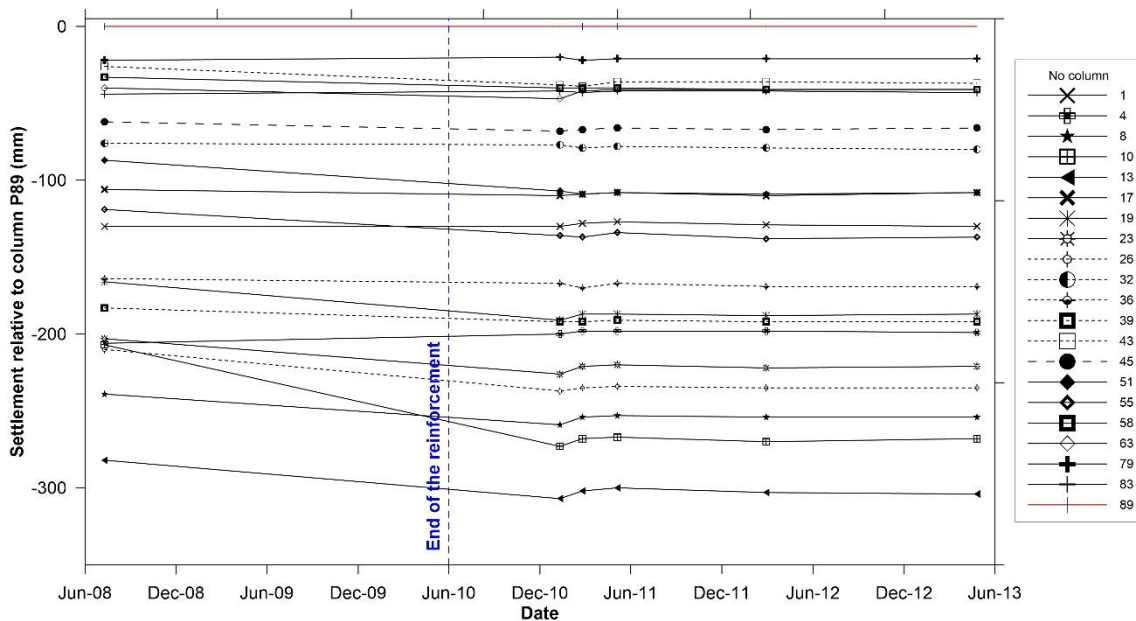
367 base of the columns of the basement floor were null or extremely small. No defined displacement

368 pattern was observed, with an average value of 2 mm (Figure 12). This order of magnitude is

369 approximately the expected absolute error for the measurement instruments. Therefore, the

370 measured displacements are not an indication of any instability of the building.

371



372

373 *Figure 12. Evolution of the relative settlement of the base of the columns. The first data corresponds to July, 2008, when the*

374 *building was settling. Note that measurements are relative to column 89. The location of columns is shown in Figure 1.*

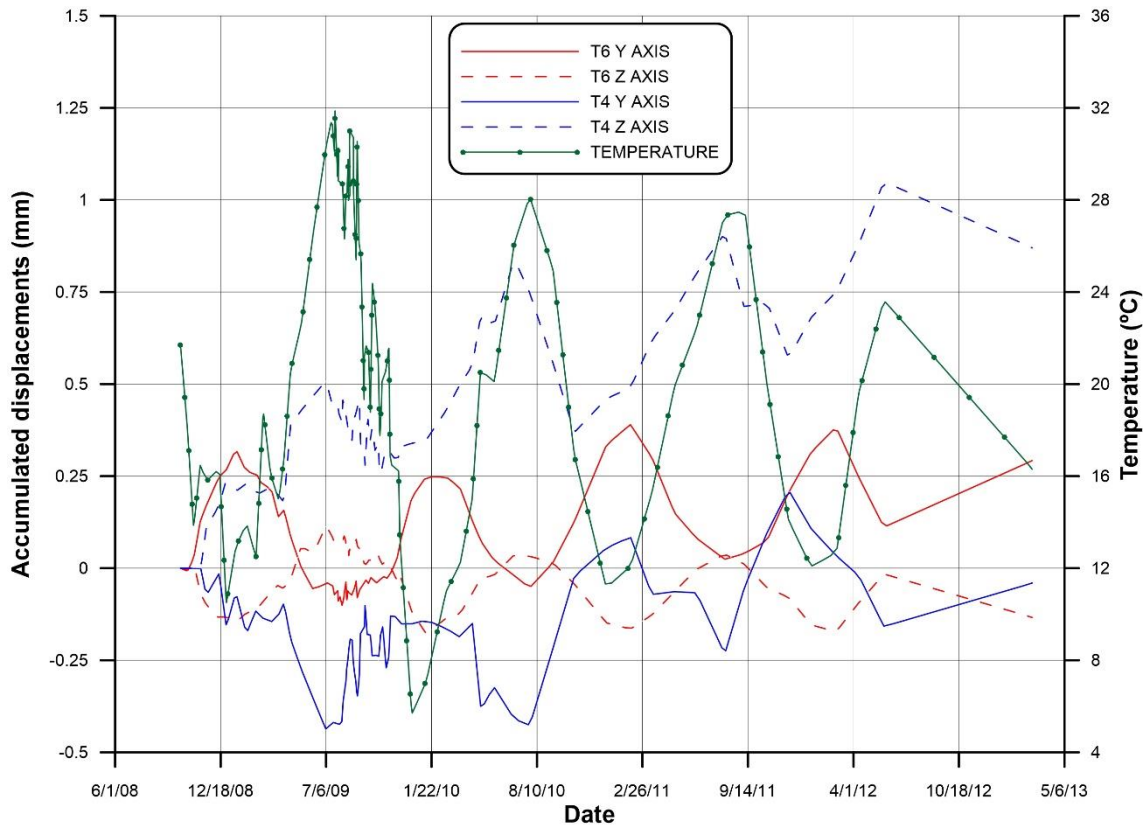
375

376 The crack monitors indicated the existence of oscillatory displacements that closed the fissures in

377 summer and opened them in winter (Figure 13). These displacements, associated with seasonal

378 temperature variations, present a main horizontal component and millimetric amplitude.

379



381

382 *Figure 13. Accumulated displacements at crack monitor n° 4 (T4) and 6 (T6). Displacements along the X-axis were zero. The*  
 383 *temperature time-series has been also represented on the plot.*

384

385 Some of the crack monitors exhibited small movements with slight increasing activity, as a result  
 386 of their function as joints and due to elastic hysteresis phenomena and fatigue of the materials.  
 387 However, these movements did not correspond to foundation movements that could cause  
 388 structural damage. These aspects are shown in Figure 13 where there is a clear relationship  
 389 between temperature (MeteoMurcia (2017)) and the displacement time series.

390

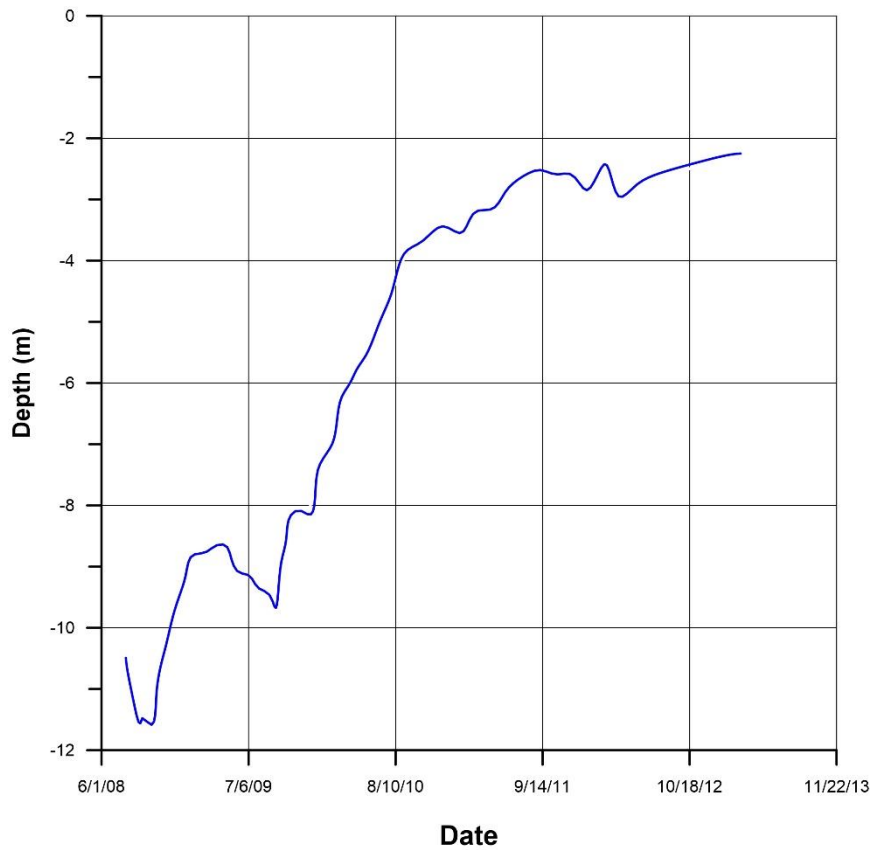


Figure 14. Time series of the groundwater level in borehole 1 (location shown in Figure 1).

391

392

393

394 Regarding the control of groundwater levels, analysis of the time series indicated the existence of  
 395 an asymptotic trend at -2.0 m depth, in accordance with pluviometry. Higher-than-average  
 396 precipitation caused fast groundwater level rise, over 8 m in 4.5 years (Figure 14). In September  
 397 2008 and 2009, two minimum precipitation records were reported (Figure 14), coinciding with  
 398 the respective annual dry seasons. Seasonal variations are not accidental and must be considered  
 399 at the time of designing the underpinning of the foundation, as occurred herein.

400 Table 5 summarizes the techniques utilized herein as well as the respective application objectives.

401

402

403

404

405

406

Investigation technique	Objectives				
	Resistant and deformational soil characterization	Groundwater level monitoring	Verification of the current state of the building	Monitoring of the building displacements	Assessment of the situation and proposals for action
Foundation study	In situ geotechnical tests	✓			✓
	Laboratory geotechnical tests	✓			✓
	Piezometer installation		✓	✓	✓
	Crack maps		✓	✓	✓
	Slab foundation levelling		✓	✓	✓
	Tilt measurements		✓	✓	✓
	Angular distortion measurement		✓	✓	✓
	Foundation inspection openings			✓	✓
	Soil-structure interaction study	FEM modelling		✓	✓
Structural study	Compilation of existing information		✓		✓
	Visual inspection		✓		✓
	Structure inspection openings		✓		✓
	2D crack monitors			✓	✓
	Crack maps		✓	✓	✓
	Concrete tests		✓		✓
	Study of the current state of the structure		✓		✓

Table 6. Data sources and investigation techniques utilized herein for forensic analysis.

407

408

409 **8. Multitechnique approach for the study and reinforcement of buildings affected by land**  
410 **subsidence.**

411

412 Considering the experience acquired in this case study, a general methodology is proposed for the  
413 study and reinforcement of buildings located on subsiding areas due to groundwater extraction.

414 The methodology consists of five steps and is illustrated in Figure 15. The first step (1<sup>st</sup> stage)  
415 consists of the compilation of existing information and first inspections. These data will lead to

416 the investigation step (2<sup>nd</sup> stage), during which the subsoil, the foundation and the structure will  
417 be characterized through the installation of devices and in situ monitoring systems (to obtain the

418 magnitude and direction of the displacements affecting the building). These displacements will  
419 be monitored throughout time during the third step (3<sup>rd</sup> stage) to determine trends and progression

420 of the displacements, which will be analysed during the fourth stage (4<sup>rd</sup> stage). Analysis of all  
421 the available information will enable a decision on the convenience of reinforcing the foundation

422 and the structure (5<sup>th</sup> stage: study of alternatives and proposals of actions). If the movements  
423 remain active after implementation of actions, monitoring will continue until the displacements



424 stop, guaranteeing the safety of the structure and verifying the appropriateness of the proposed  
425 reinforcement.

426

427 *Figure 15. Flowchart of the proposed methodology.*

428

## 429 **9. Conclusions**

430

431 Buildings located on subsiding areas are vulnerable to damage that can reduce habitability and,  
432 in some cases, jeopardize safety conditions. It is therefore necessary to formulate a general  
433 multitechnique methodology to address these specific buildings, enabling decision-making on the  
434 underpinning and/or reinforcement of these damaged structures.

435 The case study presented herein demonstrated the applicability of the proposed methodology,  
436 considering a building located in Murcia (SE Spain). The urban area of Murcia was affected by  
437 land subsidence induced by high groundwater variations caused by a long drought period and the  
438 overexploitation of the aquifer, being the first case study reported in Spain. The settlements  
439 caused by subsidence damaged more than 150 buildings (Justo and Vázquez 2002; Mulas et al.  
440 2003; Rodríguez Ortiz and Mulas 2002), among which is the case study building.

441 The damage observed was mainly due to subsidence, and was in agreement with the 10 m  
442 groundwater level drop recorded in the area between 1992 and 1995. The tilting of the building  
443 was also confirmed by the FEM model of the consolidation process. Tilting was due to the unequal  
444 thickness of the most compressible layer (Level I, silty clay), which was thicker under the main  
445 façade, and also due to the asymmetry of the loads (higher in the façade zone). This situation  
446 caused slight tilting of the structure towards the South, which was further increased by land  
447 subsidence.

448 Any heterogeneity affecting the building (e.g., asymmetry of loads, geometric asymmetry,  
449 different types and levels of foundation, etc.) can further intensify the effects of subsidence,  
450 causing serious damage to the building. Furthermore, soil heterogeneities due to changes on the  
451 thickness or properties of deformable layers under the foundation can also intensify damage.

452 Therefore, these aspects must be carefully studied and considered during the design and project  
453 phases of constructions.

454 The maximum recorded tilt for the structure was approximately 1.0%. This value is higher than  
455 the limit value established by the Spanish Technical Code ( $1/500 \cong 0.2\%$ ) (CTE 2006). The tilt  
456 of the basement columns reached maximum values of 1.67%, also exceeding the limit determined  
457 by Spanish standards (CTE 2006),  $1/250 (\approx 0.4\%)$ .

458 Regarding angular distortion, the values calculated on the date of underpinning indicated that  
459 most of the building did not present high risk of structural damage. The movement of the building  
460 followed rigid body rotation.

461 The observed damage and the recorded evolution during the monitoring period resulted in a  
462 dangerous situation, forcing the adoption of actions to stop the differential settlements of the  
463 foundation. The building foundation was underpinned with micropiles, restoring its stability and  
464 bearing capacity.

465 The cracks caused by insufficient embedment of semi resistant joists into the main beams of the  
466 first slab floor required the reinforcement of the link to avoid potential partial collapses. Steel  
467 angles were coupled to the main beam with bolts to support the semi resistant joists. Once the  
468 underpinning works were finished, aesthetics and function of the building were restored.

469 Finally, it must be noted that, in general, the underpinning solutions to be considered in buildings  
470 affected by land subsidence must ensure the transmission of loads into deep resistant layers to  
471 avoid the consolidation of more superficial layers due to groundwater level changes. However,  
472 the downward movement of soils due to consolidation processes can cause negative skin friction,  
473 inducing a drag load on the pile that must be considered in calculations.

474 The multitechnique approach proposed herein along with the reinforcement of damaged buildings  
475 has provided successful results, as demonstrated by the post-reinforcement monitoring plan.

476

#### 477 **Acknowledgments**

478 This work was supported by the Ministry of Economy and Competitiveness and EU FEDER  
479 funds, project nº TIN2014-55413-C2-2-P.

480

481 **References**

482

- 483 Aragón, R., Lambán, J., García-Aróstegui, J. L., Hornero, J., and Fernández-Grillo, A. I. (2006).  
484 "Efectos de la explotación intensiva de aguas subterráneas en la ciudad de Murcia  
485 (España) en épocas de sequía: orientaciones para una explotación sostenible." *Boletín*  
486 *Geológico y Minero*, 117, 389-400.
- 487 Burland, J. B., Broms, B. B., and De Mello, V. F. B. (1977). "Behaviour of foundations and  
488 structures." *In: Proceedings of the 9th international conference on soil mechanics and*  
489 *foundation engineering*, Japanese Society of Soil Mechanics and Foundation  
490 Engineering, 495–546.
- 491 Cooper, A. H. (2008). "The classification, recording, databasing and use of information about  
492 building damage caused by subsidence and landslides." *Quarterly Journal of Engineering*  
493 *Geology and Hydrogeology*, 41(3), 409-424.
- 494 Corapcioglu, M. Y. (1984). "Land Subsidence — A. A State-of-the-Art Review." *Fundamentals of*  
495 *Transport Phenomena in Porous Media*, J. Bear, and M. Y. Corapcioglu, eds., Springer  
496 Netherlands, Dordrecht, 369-444.
- 497 CTE (2006). "Código Técnico de la Edificación. Documento Básico de seguridad estructural -  
498 cimientos. Ministerio de Fomento de España."
- 499 Del Soldato, M., Bianchini, S., Calcaterra, D., De Vita, P., Martire, D. D., Tomás, R., and Casagli,  
500 N. (2017). "A new approach for landslide-induced damage assessment." *Geomatics,*  
501 *Natural Hazards and Risk*, 1-14.
- 502 Engineers, I. o. S. (2000). *Subsidence of Low-rise Buildings: A Guide for Professionals and Property*  
503 *Owners*, SETO Limited.
- 504 Feng, Q.-y., Liu, G.-j., Meng, L., Fu, E.-j., Zhang, H.-r., and Zhang, K.-f. (2008). "Land subsidence  
505 induced by groundwater extraction and building damage level assessment — a case  
506 study of Datun, China." *Journal of China University of Mining and Technology*, 18(4), 556-  
507 560.
- 508 Galloway, D. L., and Burbey, T. J. (2011). "Review: Regional land subsidence accompanying  
509 groundwater extraction." *Hydrogeology Journal*, 19(8), 1459-1486.
- 510 Herrera, G., Fernández, J. A., Tomás, R., Cooksley, G., and Mulas, J. (2009). "Advanced  
511 interpretation of subsidence in Murcia (SE Spain) using A-DInSAR data – modelling and  
512 validation." *Nat. Hazards Earth Syst. Sci.*, 9(3), 647-661.
- 513 Howard, H., Partners, Great, B., and Department of the, E. (1993). *Subsidence in Norwich*,  
514 H.M.S.O., London.
- 515 Hu, R. L., Yue, Z. Q., Wang, L. C., and Wang, S. J. (2004). "Review on current status and challenging  
516 issues of land subsidence in China." *Engineering Geology*, 76(1), 65-77.
- 517 Jaramillo, A., and Ballesteros, J. L. (1997). *El descenso del nivel freático en Murcia: Influencia*  
518 *sobre los edificios*, ASEMAS.
- 519 Justo, J. L., and Vázquez, N. J. (2002). *La subsidencia en Murcia: Implicaciones y consecuencias*  
520 *en la edificación*, ASEMAS, Murcia.
- 521 López Gayarre, F., Álvarez-Fernández, M. I., González-Nicieza, C., Álvarez-Vigil, A. E., and Herrera  
522 García, G. (2010). "Forensic analysis of buildings affected by mining subsidence."  
523 *Engineering Failure Analysis*, 17(1), 270-285.
- 524 MeteoMurcia (2017). "<http://www.meteomurcia.com/>."
- 525 Mulas, J., Aragón, R., Martínez, M., Lambán, J., García-Arostegui, J. L., Fernández-Grillo, A. I.,  
526 Hornero, J., Rodríguez, J., and Rodríguez, J. M. (2003). "Geotechnical and hydrological  
527 analysis of land subsidence in Murcia (Spain)." *Proc. 1st International Conference on*  
528 *Groundwater in Geological Engineering*, 50, 249-252.

- 529 Namazi, E., and Mohamad, H. (2013). "Assessment of Building Damage Induced by Three-  
530 Dimensional Ground Movements." *Journal of Geotechnical and Geoenvironmental*  
531 *Engineering*, 139(4), 608-618.
- 532 Phien-wej, N., Giao, P. H., and Nutalaya, P. (2006). "Land subsidence in Bangkok, Thailand."  
533 *Engineering Geology*, 82(4), 187-201.
- 534 Poland, J. F. (1984). "Guidebook to studies of land subsidence due to ground-water withdrawal."  
535 United Nations Educational, Scientific and Cultural Organization, Chelsea, 340.
- 536 Rodríguez Ortiz, J. M., and Mulas, J. (2002). "Subsidencia generalizada en la ciudad de Murcia  
537 (España)." *Riesgos Naturales* J. a. O. C. Ayala Carcedo, ed., Editorial Ariel, Barcelona,  
538 459–463.
- 539 Scott, R. F. (1978). "Subsidence - A review." *Evaluation and prediction of subsidence. Proc. of the*  
540 *Int. Conf., Pensacola Beach, Florida, January 1978, Am. Soc. Civil Eng., New York, 1-25.*
- 541 Tomás, R. (2009). "Estudio de la subsidencia de la ciudad de Murcia Mediante Interferometría  
542 SAR diferencial avanzada." Universidad de Alicante, Alicante.
- 543 Tomás, R., Márquez, Y., Lopez-Sanchez, J. M., Delgado, J., Blanco, P., Mallorquí, J. J., Martínez,  
544 M., Herrera, G., and Mulas, J. (2005). "Mapping ground subsidence induced by aquifer  
545 overexploitation using advanced Differential SAR Interferometry: Vega Media of the  
546 Segura River (SE Spain) case study." *Remote Sensing of Environment*, 98(2), 269-283.

547

548